

# The Nature and Significance of Solar Minima

Eric Priest

Mathematics Institute, University of St Andrews,  
St Andrews, KY16 9SS, UK  
email: [eric@mcs.st-andrews.ac.uk](mailto:eric@mcs.st-andrews.ac.uk)

**Abstract.** As an introduction to the theme of this symposium, I give a simple review of the photospheric magnetic field, the properties of the solar cycle, the way in which the magnetic field is thought to be generated by dynamo action, and finally the unusual properties of the recent solar minimum. This has awakened an interest in improving predictions of the solar cycle and in the nature of solar minima not just as gaps between maxima but as phenomena of intrinsic interest in their own right.

**Keywords.** magnetic fields, MHD, plasmas, Sun: general, Sun: magnetic fields, Sun: photosphere, sunspots

---

## 1. Introduction

Many colourful headlines have appeared in newspapers over the past 2 years, such as: the mystery of the missing sunspots; this minimum is weird; is the Sun dead? Sun shows signs of life; Earth may head into a mini-ice-age within a decade; the next ice age - now; 10 reasons to be cheerful about the coming new ice age. So what lies behind them?

As we shall discover, the solar minimum of the Sun is much more interesting than it looks at first sight. Before discussing the recent solar minimum, we need to lay the ground by describing the photospheric magnetic field, the solar cycle and dynamo activity.

## 2. The Photosphere

The Sun's radius is 700 Mm and the outer 30% of the interior is a turbulent convection zone. The atmosphere consists of the photosphere (the top of the convection zone), the chromosphere and corona.

The photosphere itself is covered with turbulent convection cells, namely, granulation on scales of 1 Mm and supergranulation on scales of 15–30 Mm. Global photospheric magnetographs reveal active regions forming a bipolar pattern of one sign in a band in the northern hemisphere and one of opposite sign in the southern hemisphere. These represent the effect of two large flux tubes below the surface, segments of which occasionally emerge through the surface to give the active regions. One flux tube is directed to the right and the other to the left.

In the core of complex active regions are to be found sunspots, but the sunspots represent only a fraction of the photospheric flux. In addition, the whole surface is covered with tiny intense flux tubes that are carried to the edges of supergranule cells and accumulated there.

In the 1980s and 90s the general picture outside active regions was of the photospheric magnetic field being mainly vertical and mainly located in supergranulation boundaries (Fig. 1). However, this paradigm has now been changed. High-resolution photospheric observations in white light show tiny bright points and lines located between granules. Furthermore, with Hinode if you reduce the threshold magnetic flux you see more and

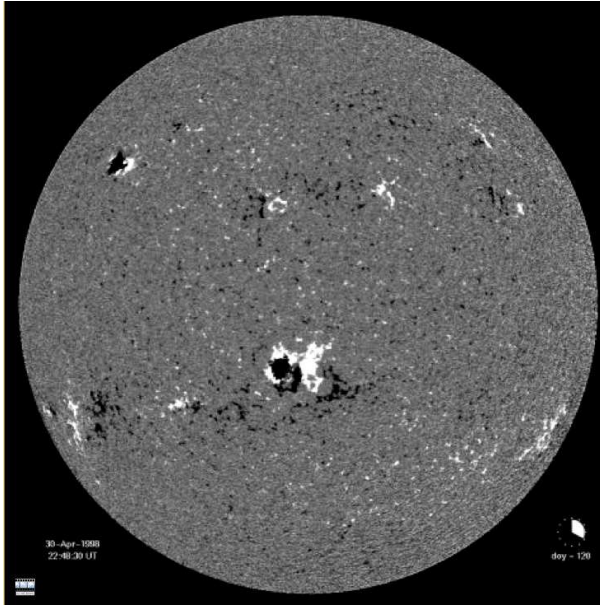


**Figure 1.** A global magnetogram of the Sun with white and black showing regions where the magnetic field is pointing towards and away from you (from the MDI instrument on the ESA/NASA SoHO spacecraft).

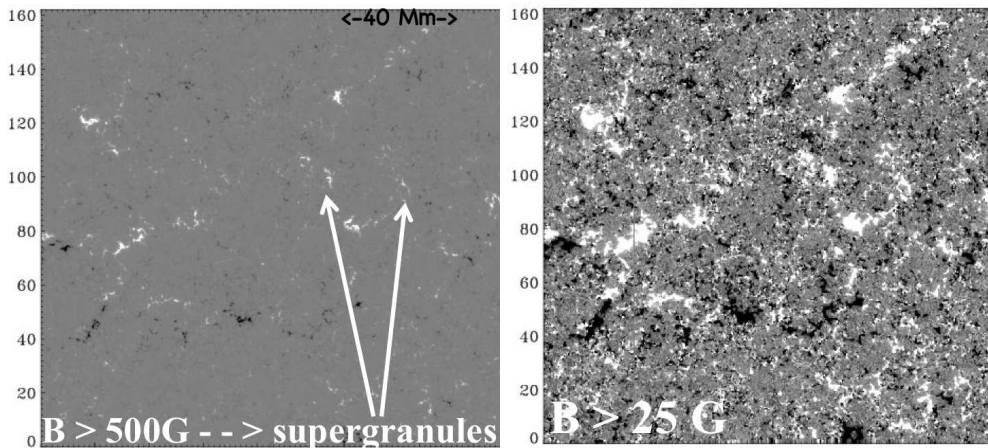


**Figure 2.** Local magnetograms of part of the quiet Sun, showing the line-of-sight when the threshold for magnetic flux is (left) 100 Gauss and (right) 25 gauss (from the Hinode spacecraft).

more line-of-sight flux, with a huge amount in the interiors of supergranules (Fig. 2). An even greater surprise was the discovery of transverse (horizontal) magnetic fields located at the edges of granules.

The Sunrise balloon mission has for the first time resolved these kilogauss vertical fields and has detected quiet-Sun magnetic fields with a flux that is lower by a factor of 10 than Hinode (i.e., down to  $2 \times 10^{15}$  Mx) (Solanki et al, 2011). Consequently, it sees ten times as many features as Hinode.

Images of sunspots from space and from the Swedish Solar Telescope show much fine structure and puzzling behaviour in the penumbra. However, impressive computational

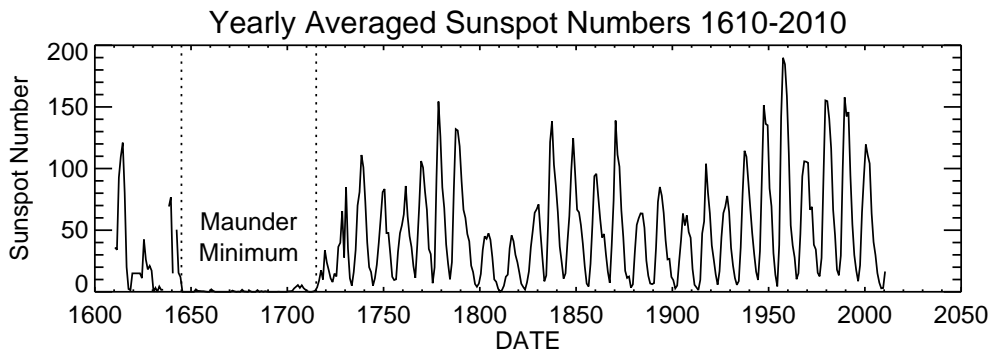


**Figure 3.** The yearly averaged sunspot number from 1610 to 2010, showing the 11-year cycle with a long-term modulation. The Maunder minimum of 1645–1715 had virtually no sunspots and the Dalton minimum of 1800–1820 had very few (courtesy David Hathaway).

models by Rempel (2011) have recently led to a breakthrough in understanding with amazingly realistic-looking images and a realisation that all the observed features are a natural consequence of convection in an inclined magnetic field.

In the convection zone, there are two important global effects of rotation on compressible turbulence. The first is the appearance of strong *differential rotation* in which the equator rotates much faster than the polar regions, having a period of 25.4 days rather than 36 days. The main driver is the Reynolds stresses ( $\langle v_r v_\phi \rangle$  and  $\langle v_\theta v_\phi \rangle$ ) which produce angular momentum fluxes. Of particular importance is the tilting of convection cells by Coriolis forces, especially in the downflowing plumes.

The second effect of rotation on turbulence is the creation of a weak *meridional flow* towards the poles at the photosphere of strength  $20 \text{ m s}^{-1}$ . This is due to small departures from magnetogeostrophic balance between large terms (namely, buoyancy, Reynolds stresses, pressure gradients and Coriolis forces) as well as small temperature differences between pole and equator.

### 3. The Solar Cycle

The number of sunspots oscillates with an 11.1-year cycle, with the period varying between 8 and 15 years and the maximum varying substantially. When the rise phase is faster then the cycle tends to be larger and longer. Also, there is a long-term modulation known as the Gleissberg cycle. Around 1910, 1810 and 1710 the maxima were smaller than average and the minima deeper (see talks by Svalgaard and Miyahara).

Jack Eddy realised that there were hardly any sunspots at all in most of the 17th century (Fig. 3), a period of 70 years from 1645 to 1715 known as the *Maunder minimum*. This period was also known as the Little Ice Age, since the climate of Europe was considerably cooler than normal with the river Thames occasionally freezing over. Detailed sunspot numbers started in 1750, but solar cycle variations can also be seen much further back for 30,000 years in  $^{10}\text{Be}$  ice cores and  $^{14}\text{C}$  tree rings (see the talks by Saar and Usoskin).

So, how typical is the current solar cycle behaviour? Well it depends how far you look – looking back 400 years the current modern maximum is unusual (but see L Svalgaard’s presentation here). However, looking back say 10,000 years, the recent maximum and minimum are very common and in fact 9000 years ago the maxima were considerably greater than the recent maxima.

It is interesting to note that the  $^{10}\text{Be}$  oscillation continues through the Maunder min-

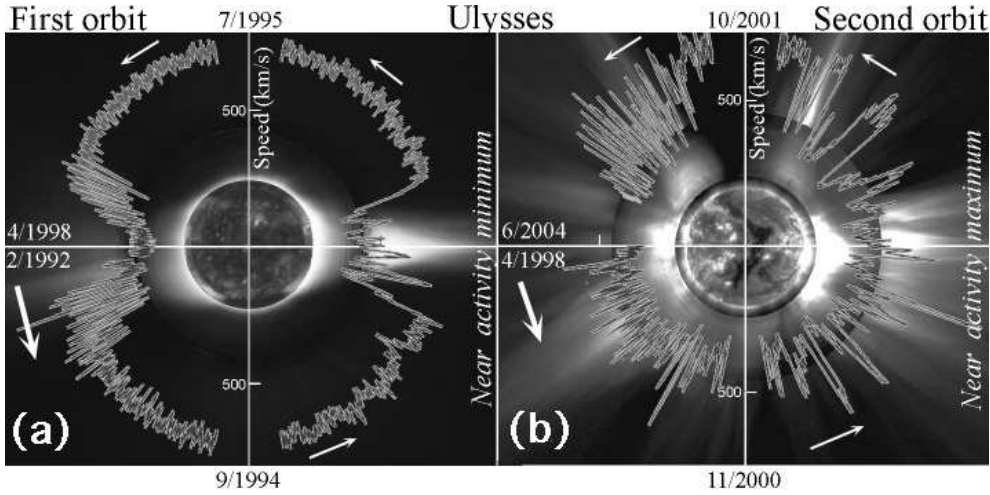


**Figure 4.** Solar wind speed as a function of latitude in a polar plot from the ULYSSES spacecraft during (a) solar minimum and (b) solar maximum. Superimposed are coronal images from the Mauna Loa K coronameter, plus SoHO EIT and LASCO. (From Meyer, 2007).

imum, so that the magnetic cycle did not switch off but just reduced in strength so that sunspots could not form readily (Beer et al, 1998). Furthermore, it has recently been shown that the decline into the Maunder minimum was gradual rather than sudden (Vaquero, 2011). The cause of the Maunder minimum may be *intermittency*, when there is a random change from one state of behaviour to another. This may be due to stochastic noise, nonlinearities, threshold effects or time delays (e.g., Charbonneau, 2010).

During the solar cycle the whole solar atmosphere varies, not just the sunspot number. For example, the chromosphere has quite a different appearance at solar minimum and solar maximum, as does the global magnetic field revealed in white-light eclipse images: thus, at solar minimum the corona has a dipole shape with prominent open plumes at the poles and helmet streamers at the equator, whereas at solar maximum the corona is much more isotropic with streamers stretching out from all latitudes (see the talks by Tlatov and Vasquez). Furthermore, the coronal intensity in soft x-rays increases by a factor of a hundred from minimum to maximum. In addition, the corona is much more highly structured and varied at solar maximum.

The solar wind velocity varies with the solar cycle. At a normal solar minimum, there are long-lasting fast solar wind streams of  $700 \text{ km s}^{-1}$  spreading over a large angle from both poles and sporadic slow solar wind at  $300 \text{ km s}^{-1}$  from large equatorial streamers (Fig. 4a). At solar maximum, the corona is much more isotropic with mixed fast and slow streams at all latitudes (Fig. 4b). As we shall see in this conference, the present solar minimum has a very different appearance from normal (see talk by de Toma). The interplanetary open magnetic flux also varies with the cycle and was much lower than normal in the recent solar minimum. Again, along with the variations in active regions, the solar cycle produces an oscillation in the locations and frequency of solar flares, prominences and coronal mass ejections (see the talks by Cliver, Cremades, Webb, Bothmer, Gibson).

Magnetic butterfly diagrams such as Fig. 5 are highly revealing. They show how the sunspots migrate equatorward during the solar cycle, and indicate the polewards migration of trailing flux, especially near sunspot maximum. This leads to a reversal of the polar field about a couple of years after maximum, which is also clearly visible.

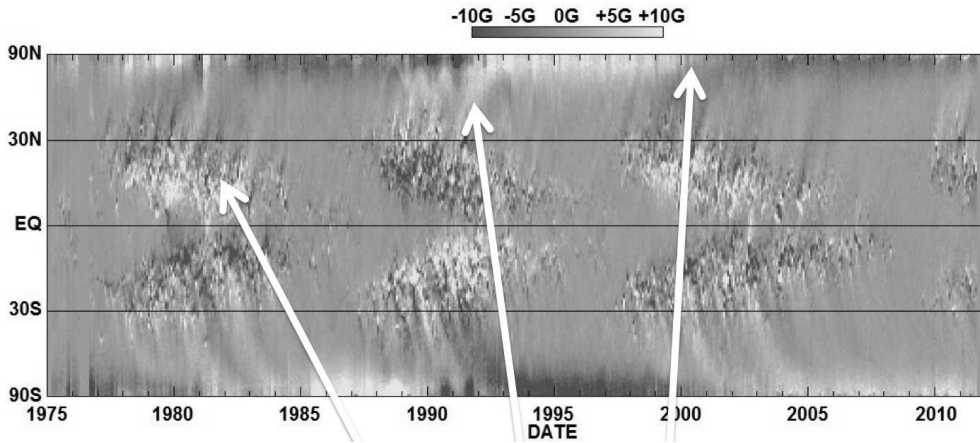


**Figure 5.** A magnetic butterfly diagram showing the variation in sunspots of positive (light) and negative polarity (dark) as a function of time from 1975. A series of arrows (from left to right) indicate: the migration of sunspots towards the equator; the poleward migration of trailing flux by a meridional flow; and the reversal of the polar field about 2 years after sunspot maximum. (Courtesy D Hathaway).

Finally, there are many effects of the solar cycle at Earth, including aspects of space weather, geomagnetic activity, cosmic rays, the Earth's atmosphere and climate (see talks by Luhmann, Echer, Kazuoki, Munakata, Rozanov, Batista, Guhathakurta, Mendoza and Bertucci). Indeed, Lockwood (2010) has shown that the Sun cannot be the main cause of the present increase in the global temperature of the Earth, since currently the effect of the Sun is declining rather than increasing. Also, Feulner (2010) has estimated that, even if a Maunder minimum were taking place just now, its effect would be to decrease the global temperature by only 0.3 °C by 2100, which is far smaller than the temperature increase expected from greenhouse gases emitted by humans.

#### 4. Generating the Magnetic Field by a Dynamo

The dynamo problem is an interesting nonlinear example of regular behaviour with turbulent or chaotic aspects. After Cowling (1934) had shown that generating an axisymmetric magnetic field is impossible, Parker (1955a, 1955b) made conceptual breakthroughs by showing how flux tubes rise by *magnetic buoyancy* and by suggesting how both the toroidal and poloidal field components ( $B_{tor}$ ,  $B_{pol}$ ) could be generated. His idea was that differential rotation generates a toroidal field from a poloidal field (the  $\omega$ -effect) and turbulent cyclonic convection in turn generates poloidal field from a toroidal one (the  $\alpha$ -effect) (Fig. 6). He modelled the latter process by a term of the form  $\nabla \times (\alpha \mathbf{B})$ , although he used the notation  $\Gamma$  in place of  $\alpha$ . This physical idea was formalised as *mean-field theory* by Steenbeck et al (1966) and Moffatt (1978), who wrote the magnetic field as the sum of a large-scale mean field and a small-scale turbulent field in the MHD equations. A key result of the theory is that an angular velocity that increases with depth ( $d\Omega/dr < 0$ ) is required to give migration of dynamo activity towards the equator.

In the 1980's, cracks started appearing in the above framework for producing  $B_{pol}$  by the  $\alpha$ -effect, although the  $\omega$ -effect remains accepted to this day as the mechanism for generating  $B_{tor}$ . It was realised that the properties of emerging fields, such as the latitudes of emergence and the tilts of bipoles, require fields of  $10^5$  Gauss, but these would rise through the convection zone very quickly and would be resistant to turbulence, so

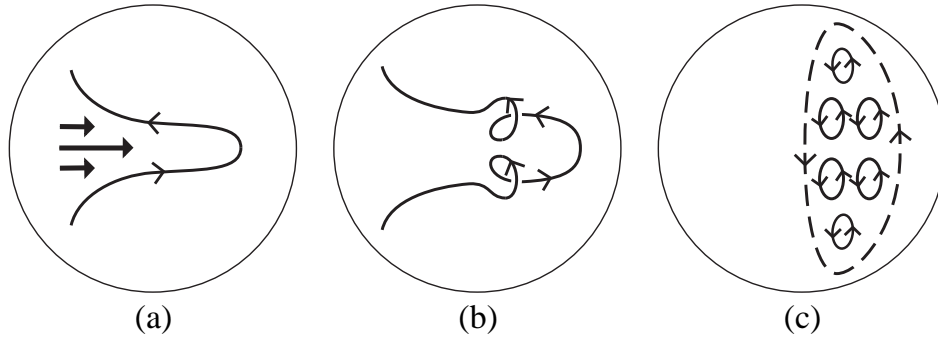


**Figure 6.** Parker’s dynamo model in which: (a) toroidal flux is generated from poloidal flux by differential rotation (the  $\omega$ -effect); (b) the effect of two helically rising blobs on the toroidal field; (c) the merging of the resulting closed loops of many cyclonic eddies to give new large-scale (dashed) poloidal flux (the  $\alpha$ -effect).

that the  $\alpha$ -effect would stall. Also, global simulations failed to give solar-like dynamos and doubts appeared about the validity of mean-field theory and the derivation of the  $\alpha$ -effect, in particular the assumption that the fluctuating fields are much smaller than the mean field.

However, the final nail in the coffin of the previous theory appeared when helioseismology showed that the angular velocity is constant with radius ( $d\Omega/dr = 0$ ) in the convection zone rather than increasing outwards as required by the theory. It had long been known that the solar rotation at the surface increases from poles to equator and had been expected that in the solar interior the rotation would be constant on cylinders and the magnetic field would be generated throughout the convection zone. Surprises from helioseismology were that the angular velocity is instead constant on cones and that the rotation below the convection zone is uniform, so that there is a strong shear layer, called the *tachocline*, at the base of the convection zone. This is now thought to be the site of the main dynamo that produces active regions and sunspots. However, there may well be another dynamo just below the photosphere that generates the small-scale magnetic field seen in ephemeral regions and intense flux tubes at the edges of granules and supergranules.

In the 1990’s, two new ideas were proposed for generating a poloidal field from a toroidal one (Fig. 7). The first is by some kind of *tachocline dynamo* at the tachocline, namely, either locating both the  $\alpha$ -effect and  $\omega$ -effect in the overshoot region just below the base of the tachocline or in an interface dynamo separating these effects spatially and placing the  $\omega$ -effect below the interface and the  $\alpha$ -effect above it (Parker, 1993, Charbonneau, 1978). The second idea was to propose a *flux-transfer dynamo* that develops the earlier Babcock (1961)-Leighton (1969) dynamo by solving the axisymmetric kinematic dynamo equations with an imposed meridional flow and an  $\omega$ -effect focussed near the tachocline together with an  $\alpha$ -effect at the solar surface (Choudhuri, 1995; Dikpati, 1994; Charbonneau, 1997; Nandi, 2001).

Many other effects are potentially important in dynamo theories, such as: shear instabilities, magnetic buoyancy instabilities, flux tube instabilities in the tachocline or the overshoot layer; the back-reaction of the Lorentz force on the flow and the efficiency of the  $\alpha$ -effect; time delays or stochastic forcing to modulate the dynamo; and a proper treatment of sub-grid physics in numerical experiments (see the talk by Brun and the living review by Charbonneau (2010)).

Full MHD global computations have been conducted by a number of authors, including

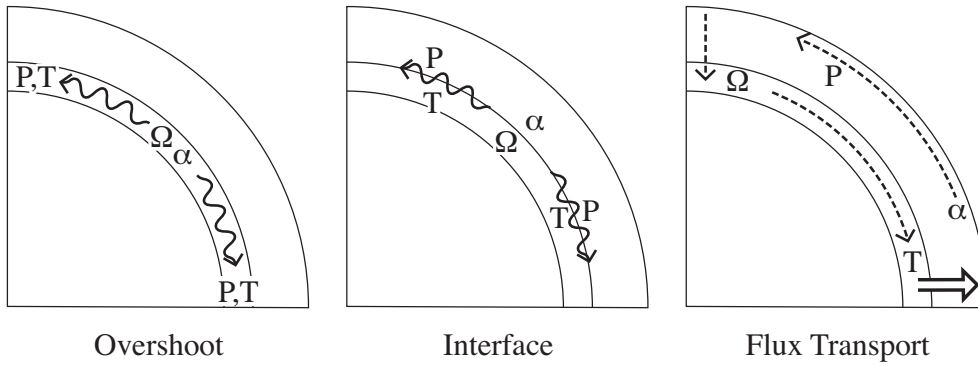


**Figure 7.** Magnetic field generation by overshooting, interface and flux-transport dynamos, indicating where the  $\alpha$ - and  $\omega$ -effects are located and where poloidal (P) and toroidal (T) components are generated. Curly, dashed and double arrows represent transport by a dynamo wave, meridional flow and buoyant flux emergence, respectively.

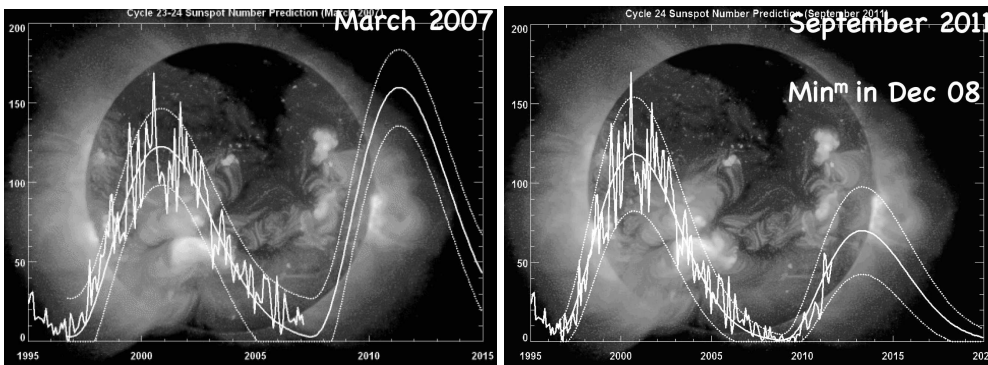


**Figure 8.** Predictions of the future sunspot number in (a) March 2007 and (b) September 2011 (Courtesy D Hathaway).

Brun (2004) and Ghizaru (2010). They are now able to resolve supergranulation and generate reasonable behaviour for differential rotation and meridional circulation, as well as a turbulent  $\alpha$ -effect and reversals of the magnetic fields (see talks by Brandenburg and Browning).

Predicting the solar cycle is, however, a tough endeavour. Many methods have been employed, including climatological effects, dynamo theory, neural networks, polar fields and geomagnetic indices. The maximum sunspot numbers predicted for cycle 24 have ranged between 40 and 170 among the 75 or so attempts. For example, flux transport dynamo theory has been used by Dikpati et al (2006) and Choudhuri et al (2007). They adopted different values for the magnetic diffusivity, differential rotation, meridional circulation, poloidal flux source and alpha quenching. The former predicted a strong cycle with a maximum of about 140, whereas the latter predicted a weak cycle with a maximum of about 80. David Hathaway is one of the experts at predictions and the way in which his predictions have varied in time is illustrated in Fig. 8.

## 5. How has this Solar Minimum been Different?

The present solar minimum has been unusual in many ways. The sunspot number (Fig. 9) illustrates how the decline in sunspot number into the minimum was much more

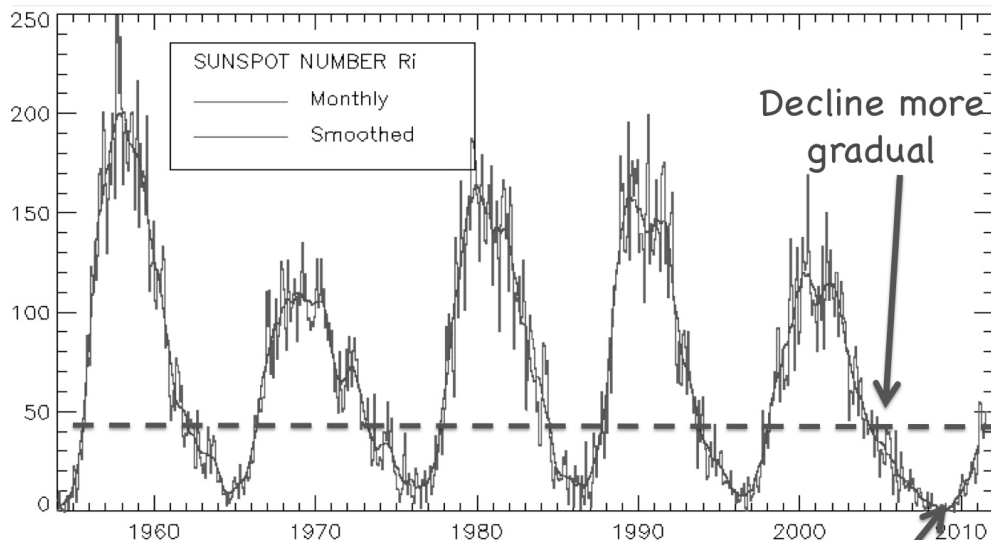


**Figure 9.** The recent sunspot number, indicating the slow decline into the minimum and the depth and length of the minimum (Courtesy R Van der Linden, Solar Influences Data Centre, Brussels).

gradual and how the minimum itself was much deeper and longer than in the previous few cycles. In 2008, 75% of the days were spotless, whereas in 2009 this figure rose to 90%. The duration of the last cycle was 12.6 years, the longest for 100 years and the next maximum could well be the lowest for 200 years.

The butterfly diagram shows that usually the cycles overlap, with the new sunspots appearing at high latitudes at the start of a new cycle at the same time as spots from the old cycle are still appearing at low latitudes. However, this was not the case this time, since a clear gap between the two cycles has been present. The same was true back in 1900. The magnetic butterfly diagram also shows how the sunspots have approached the equator much more slowly in the last cycle and the polar fields have been much weaker.

The mean interplanetary open magnetic flux varies with the cycle, and its value at solar minimum fell from  $3.82 \times 10^{16}$  Wb in 1987 to  $1.98 \times 10^{14}$  Wb in 2007 (Lockwood et al, 2009). (See the talks by de Toma and Dasso for the way the global and interplanetary fields have varied.)

For sunspots, their brightness varies in phase with the solar cycle, while their radius is independent of the cycle. Recently, Livingston and Penn (2009) have suggested that the magnetic field strength in sunspots is weakening by 50 Gauss per year. If the variation is a straight line and continues in future, they point out that it will fall below the value of 1500 Gauss needed for sunspots to form in 2020. However, there is a large scatter in the data, which may also be fit by a curve that reaches a minimum in future and then increases.

Furthermore, the total solar irradiance has been lower during the recent minimum than in the previous two (see talk by Schmutz), although the mechanism is unclear.

An intriguing recent discovery is that differential rotation varies with the solar cycle, as shown in Fig.10. Alternating bands of rotation that are faster and slower than normal are located polewards of the active-region belts and migrate from mid-latitudes towards the equator. By comparison with the previous cycle, the polar branch has been late starting at this minimum (see talk by Thompson). The meridional flow varies too: Mount Wilson observations for the last two cycles show that during cycle 22 there was a counter-flow

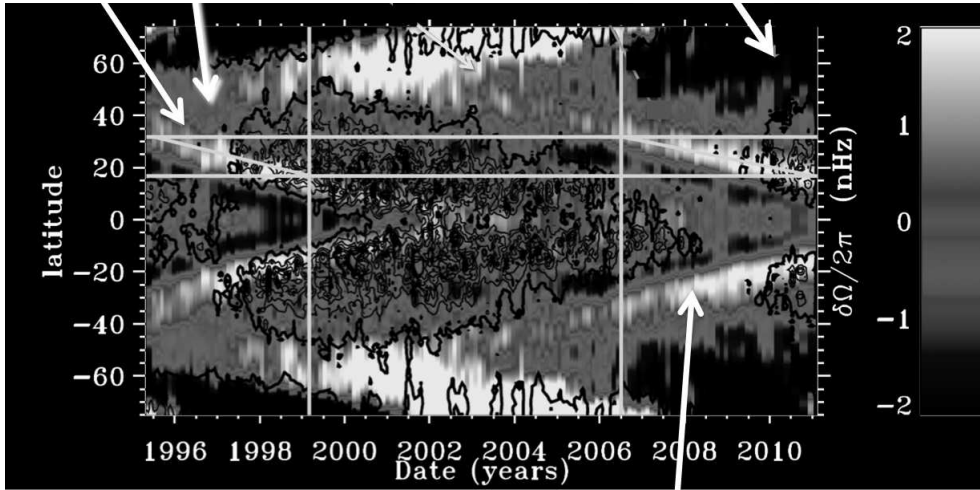


**Figure 10.** Torsional oscillations showing alternating bands rotating faster and slower than normal, the migration of the bands from mid-latitudes to equator and the fact that the polar branch is late in starting (Courtesy Rachel Howe).

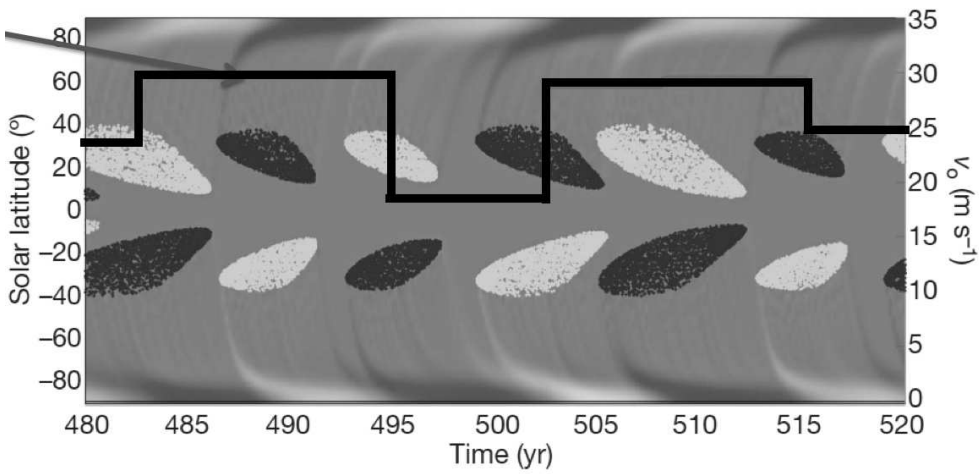


**Figure 11.** A butterfly diagram produced by a flux-transport model in which the meridional flow is imposed to vary in a manner indicated by the dark black line (Courtesy Dibyendu Nandi).

away from the poles as well as the normal flow towards the poles, whereas in cycle 23 there was no counter-flow. Although meridional flow can so far be measured only in the top 15 Mm of the convection zone, this suggests that perhaps the meridional flow formed a double-cell pattern in cycle 22 but a single-cell pattern in cycle 23 (Dikpati, 2010).

The effect of a variable meridional flow on flux transport dynamos has been evaluated by Nandi, Munoz and Martens (2010). Their simulated butterfly diagram (Fig.11) indicates how a fast meridional flow produces no overlap in cycles, whereas a slow flow makes the cycles overlap. What happens in their scenario is that the value of the flow in the rise phase affects the cycle overlap and the polar field at solar minimum. Thus, a fast meridional flow sweeps the poloidal field more rapidly along the base of the tachocline, so that a weaker toroidal field is built up, leading to a smaller sunspot cycle.

## 6. Conclusion

For the solar dynamo, great progress has been made over the past few years with many new ideas. There is a healthy tension between the pure dynamo theorists, who for example wonder about the validity of mean-field theory, and the applied dynamo theorists who are more motivated by an attempt to explain observed features of the solar cycle. Clearly, both approaches are needed for a full understanding. However, many aspects are unclear: where and by what kind of alpha-effect is the toroidal field converted into poloidal flux? what is the relation between sunspots and the strength of a magnetic cycle? what value should be put on the strength of the turbulent magnetic diffusivity?

For the solar cycle, it is not clear what is the best way of defining solar minimum. Also, it is a challenge to be able to predict the values and dates of the next solar maximum and solar minimum. When will the next Maunder minimum take place? Also, what is the precise effect of the Sun on the Earth's climate?

Furthermore, the present solar minimum has revealed many unusual features that highlight fundamental problems in understanding about the nature of the dynamo and the solar cycle. I look forward with great anticipation to hearing the latest results and ideas during this symposium and hopefully to Karel Schrijver's answers to some of our questions. In the meantime, let's have fun showing just how interesting the solar minimum is.

## References

- Babcock, H. W. (1961). The topology of the Sun's magnetic field and the 22-year cycle. *Astrophys. J.* **133**, 572–587.
- Beer, J., Tobias, S., and Weiss, N. O. (1998). An active Sun throughout the Maunder minimum. *Solar Phys.* **181**, 237–249.
- Brun, A. S., Miesch, M. S., and Toomre, J. (2004). Global-scale turbulent convection and magnetic dynamo action in the solar envelope. *Astrophys. J.* **614**, 1073–1098.
- Charbonneau, P. and MacGregor, K. B. (1997). Solar interface dynamos: II - Linear, kinematic models in spherical geometry. *Astrophys. J.* **486**, 502–520.
- Charbonneau, P., Beaubien, G., and St-Jean, C. (2007). Fluctuations in Babcock-Leighton dynamos. II. Revisiting the Gnevyshev-Ohl rule. *Astrophys. J.* **658**, 657–662.
- Charbonneau, P. (2010). Dynamo models of the solar cycle. *Living Reviews in Solar Physics* **7**, 3.
- Choudhuri, A. R., Schüssler, M., and Dikpati, M. (1995). The solar dynamo with meridional circulation. *Astron. Astrophys.* **303**, L29–L32.
- Choudhuri, A. R., Chatterjee, P., and Jiang, J. (2007). Predicting solar cycle 24 with a solar dynamo model. *Phys. Rev. Letts.* **98**, 131,103–131,107.
- Cowling, T. G. (1934). The magnetic field of sunspots. *Mon. Not. Roy. Astron. Soc.* **94**, 39–48.
- Dikpati, M. and Choudhuri, A. R. (1994). The evolution of the Sun's poloidal field. *Astron. Astrophys.* **291**, 975–989.
- Dikpati, M. and Gilman, P. A. (2006). Simulating and predicting solar cycles using a flux-transport dynamo. *Astrophys. J.* **649**, 498–514.
- Dikpati, M., Gilman, P. A., and Ulrich, R. K. (2010). Physical origin of differences among various measures of solar meridional circulation. *Astrophys. J.* **722**, 774–778.
- Feulner, G. and Rahmstorf, S. (2010). On the effect of a new grand minimum of solar activity on the future climate on Earth. *Geophys. Res. Lett.* **370**, L05707.
- Ghizaru, M., Charbonneau, P., and Smolarkiewicz, P. K. (2010). Magnetic cycles in global large-eddy simulations of solar convection. *Astrophys. J. Letts.* **715**, L133–L137.
- Howe, R., Hill, F., Komm, R., Christensen-Dalsgaard, J., Larson, T. P., Schou, J., Thompson, M. J., and Ulrich, R. (2011). The torsional oscillation and the new solar cycle. *Journal of Physics Conference Series* **271**, 1 (Jan.), 012074.
- Leighton, R. B. (1969). A magneto-kinematic model of the solar cycle. *Astrophys. J.* **156**, 1–26.

- Livingston, W. and Penn, M. (2009). Are sunspots different during this solar minimum? *EOS Transactions* **90**, 257–258.
- Lockwood, M., Owens, M., and Rouillard, A. P. (2009). Excess open solar magnetic flux from satellite data: 2. A survey of kinematic effects. *J. Geophys. Res.* **114**, A111014.
- Lockwood, M., Harrison, R. G., Woollings, T., and Solanki, S. K. (2010). Are cold winters in Europe associated with low solar activity? *Environmental Research Letters* **5**, 2 (Apr.), 024001.
- Meyer-Vernet, N. 2007, *Basics of the Solar Wind*, Cambridge University Press (Cambridge UK)
- Moffatt, H. K. (1978). *Magnetic Field Generation in Electrically Conducting Fluids*. (Cambridge University Press, Cambridge, England).
- Muñoz-Jaramillo, A., Nandy, D., and Martens, P. C. H. (2009). Helioseismic data inclusion in solar dynamo models. *Astrophys. J.* **698**, 461–478.
- Muñoz-Jaramillo, A., Nandy, D., Martens, P. C. H., and Yeates, A. R. (2010). A double-ring algorithm for modeling solar active regions: Unifying kinematic dynamo models and surface flux-transport simulations. *Astrophys. J. Letts.* **720**, L20–L25.
- Nandy, D. (2006). Magnetic helicity and flux tube dynamics in the solar convection zone: Comparison between observation and theory. *J. Geophys. Res.* **111**, A12S01.
- Nandy, D. and Choudhuri, A. R. (2002). Explaining the latitudinal distribution of sunspots with a deep meridional flow. *Science* **296**, 1671–1673.
- Nandy, D., Muñoz-Jaramillo, A., and Martens, P. C. H. (2011). The unusual minimum of sunspot cycle 23 caused by meridional plasma flow variations. *Nature* **471**, 80–82.
- Parker, E. N. (1955a). The formation of sunspots from the solar toroidal field. *Astrophys. J.* **121**, 491–507.
- Parker, E. N. (1955b). Hydromagnetic dynamo models. *Astrophys. J.* **122**, 293–314.
- Parker, E. N. (1993). A solar dynamo surface wave at the interface between convection and nonuniform rotation. *Astrophys. J.* **408**, 707–719.
- Rempel, M. (2011). Penumbra fine structure and driving mechanisms of large-scale flows in simulated sunspots. *Astrophys. J.* **729**, 5.
- Solanki, S. K., Barthol, P., Danilovic, S., Feller, A., Gandorfer, A., Hirzberger, J., Riethmüller, T. L., Schüssler, M., Bonet, J. A., Martínez Pillet, V., del Toro Iniesta, J. C., Domingo, V., Palacios, J., Knölker, M., Bello González, N., Berkefeld, T., Franz, M., Schmidt, W., and Title, A. M. (2010). SUNRISE: Instrument, mission, data, and first results. *Astrophys. J. Letts.* **723**, L127–L133.
- Steenbeck, M., Krause, F., and Rädler, K. H. (1966). Berechnung der mittleren Lorentz-Feldstärke  $\overline{\mathbf{v} \times \mathbf{B}}$  für ein elektrisch leitendes Medium in turbulenter, durch Coriolis-Kräfte beeinflusster Bewegung. *Z. Naturforsch* **21a**, 369–376.
- Vaquero, J. M., Gallego, M. C., Usoskin, I. G., and Kovaltsov, G. A. (2011). Revisited sunspot data: A new scenario for the onset of the Maunder minimum. *Astrophys. J. Letts.* **731**, L24.

## Discussion

THOMPSON:

PRIEST: